# Subcritical wave instability in reaction-diffusion systems

Vladimir K. Vanag and Irving R. Epstein
*Department of Chemistry and Volen Center for Complex Systems, MS 015, Brandeis University, Waltham, Massachusetts 02454-9110*

(Received 12 March 2004; accepted 20 April 2004)

We report an example of subcritical wave instability in a model of a reaction-diffusion system and discuss the potential implications for localized patterns found in experiments on the Belousov-Zhabotinsky reaction in a microemulsion. © *2004 American Institute of Physics.*
[DOI: 10.1063/1.1760742]

## I. INTRODUCTION

Pattern formation in reaction-diffusion systems induced by small-amplitude perturbations of the homogeneous steady state typically involves one of the two diffusive instabilities: the Turing and the wave instabilities.[1,2] The Turing instability is characterized by $\mathrm{Re}(\Lambda)>0$ and $\mathrm{Im}(\Lambda)=0$, where $\Lambda$ is an eigenvalue of the Jacobian matrix, for some finite range of wave numbers $k>0$. The patterns generated are stationary in time and periodic in space.[2] The wave instability, sometimes referred to as the finite wavelength instability, is characterized by $\mathrm{Re}(\Lambda)>0$ and $\mathrm{Im}(\Lambda)\neq 0$ in a finite range of $k>0$ and gives rise to patterns periodic both in time and in space,[2] realized either as standing[3] or as packet waves.[4] The Turing instability has been analyzed in considerable detail,[5,6] but the properties of the wave instability have not been characterized as fully, despite the fact that this latter instability can produce a wealth of complex patterns including, for example, antispirals[7] and accelerating waves.[8]

The Hopf bifurcation, which leads to homogeneous bulk oscillations, and the Turing instability can be either supercritical or subcritical.[9–11] A subcritical Turing instability, which requires a large-amplitude perturbation, can lead to localized stationary patterns.[12–14] A combination of subcritical Turing and subcritical Hopf instabilities can produce oscillons,[14] localized oscillatory nonmoving spots. It seems reasonable that the wave bifurcation might also occur subcritically, but we are unaware of prior reports or discussions of subcritical wave instability (SWI) in reaction-diffusion systems. Here we report an example of SWI in a simple model of a reaction-diffusion system, analyze the system behavior above and below the supercritical bifurcation point, and comment on the possible relevance of SWI to experiments on the Belousov-Zhabotinsky reaction dispersed in water-in-oil AOT microemulsion (BZ-AOT system).

## II. A MODEL FOR SWI

We suggest here a method for generating SWI that, while not generic, may still be useful given the lack of other approaches, since it should work in many, though not all, cases. We start with a two-variable reaction-diffusion model that possesses a subcritical Hopf instability (SHI). Next, we add a third variable linearly coupled with the activator (autocatalytic) variable of our initial model. This augmentation procedure has been found to generate (supercritical) wave instability in several three-variable models.[4,15] Our motivation is that the character of the SHI at wave number $k=0$ may carry over to the wave instability at nonzero wave number $k_0$, where the real part of the most positive eigenvalue of the Jacobian matrix has a maximum (see Fig. 1).

For specificity, we investigate the following extended Oregonator[16–18] model:

$$dx/dt=[x(1-x)-fz(x-q)/(x+q)-\beta x+s]/\varepsilon + D_x\Delta x, \tag{1}$$

$$dz/dt=x-z+D_z\Delta z, \tag{2}$$

$$ds/dt=(\beta x-s)/\varepsilon_2+D_s\Delta s, \tag{3}$$

where $x$ and $z$ represent normalized dimensionless concentrations of the activator ($HBrO_2$) and the catalyst $[Fe(phen)_3^{2+}]$, respectively. If $q$ is small (e.g., $q=0.002$), $f<1-q$, and $\beta=0$, the basic two-variable model (1,2) exhibits SHI.[17] For small $\beta$, introducing the new variable $s$ ($s$ in the BZ-AOT system represents the radical $BrO_2^*$ in the oil phase) does not destroy the SHI, though the values of $\varepsilon$ at the onset of both the supercritical and subcritical Hopf instabilities, $\varepsilon_H$ and $\varepsilon_{SH}$, respectively, change slightly. The parameter range for SHI is narrow; $(\varepsilon_{SH}-\varepsilon_H)/\varepsilon_H\cong 0.0011$. For values of $\varepsilon>\varepsilon_{SH}$, only the steady state is stable for the homogeneous, well-mixed (point) system (1–3). Linear stability analysis reveals that when $D_x=D_z\ll D_s$, system (1–3) can exhibit wave instability for both small and large $\beta$. By slightly increasing $\beta$ and tuning the other parameters ($\varepsilon$, $f$, and/or $D_s$), we can find a parameter range in which SWI occurs (region between curves 1 and 2 in Fig. 2), as demonstrated by computer simulations.

We integrated the partial differential equations (1)–(3) using the FLEXPDE package, in which a Newton-Raphson iteration process is used with a variable time step and mesh. FLEXPDE refines the triangular finite element mesh and/or time step until the estimated error in any variable is less than a specified tolerance, which we chose as $10^{-4}$ at every cell of the mesh. Larger tolerances, such as $10^{-3}$, also give good agreement between the lines of supercritical wave bifurcation found computationally and calculated by linear stability analysis. We employed the smaller tolerance for more accurate determination of the range of subcriticality.

 

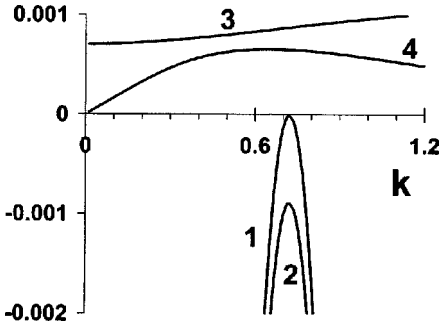


FIG. 1. Dispersion curves for subcritical wave instability obtained by linear stability analysis of model (1–3): curves 1 and 2 are $\mathrm{Re}(\Lambda)$ at $\varepsilon=0.3466$ and 0.3472, respectively; curve 3 is $\mathrm{Im}(\Lambda)/1000$ (the curves are indistinguishable for these two values of $\varepsilon$); and curve 4 is $[d\ \mathrm{Im}(\Lambda)/dk]/500$. Parameters: $q=0.002$, $f=0.92$, $\beta=0.4$, $\varepsilon_2=1.2$, $D_x=D_z=0.1$, and $D_s=1$.

The amplitude of standing waves serves as a useful parameter for quantitative control of subcritical and supercritical WI. With SWI and positive $\mathrm{Re}(\Lambda)_{\max}$, if we start from a small sinusoidal initial perturbation of the homogeneous steady state in one spatial dimensional with zero-flux boundary conditions, the amplitude of oscillation grows exponentially with a rate $\mathrm{Re}(\Lambda)_{\max}$ and then reaches a stationary amplitude $A$ (Fig. 3), which is determined by the nonlinear terms in model (1–3). If, by varying $\varepsilon$, we then move to the point of supercritical bifurcation, $\varepsilon_W$, where $\mathrm{Re}(\Lambda)_{\max}=0$, and beyond this point to negative $\mathrm{Re}(\Lambda)_{\max}$, the amplitude of the standing waves decreases slightly, but the standing waves survive in a range of negative $\mathrm{Re}(\Lambda)_{\max}$, so long as $\varepsilon_W<\varepsilon<\varepsilon_{SW}$ (Fig. 4). We note that the relative ranges over which SWI and SHI occur are roughly equal: $(\varepsilon_{SW}-\varepsilon_W)/\varepsilon_W \cong (\varepsilon_{SH}-\varepsilon_H)/\varepsilon_H$.

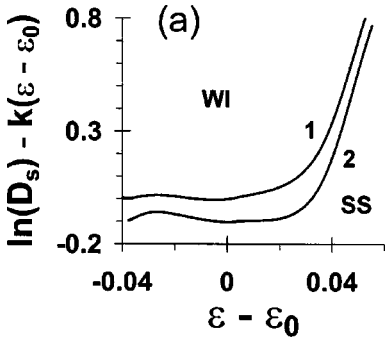


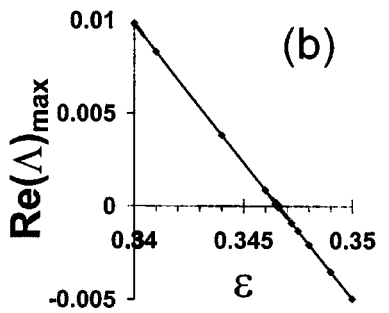


FIG. 2. (a) Phase diagram in the $D_s$-$\varepsilon$ plane. Region of subcritical wave instability lies between curves 1 and 2. Curve 1 (supercritical bifurcation) is obtained both analytically (by linear stability analysis) and by computer simulations of model (1–3). Curve 2 (subcritical bifurcation) is obtained by computer simulations only. WI is region of supercritical wave instability. SS is steady state. Fixed parameters of model (1–3) as in Fig. 1, $\varepsilon_0=0.346\,58$ [value of $\varepsilon$ at which $\mathrm{Re}(\Lambda)=0$ at $D_s=1$], $k=25$ (arbitrary coefficient chosen for clearer viewing of curves 1 and 2); (b) Linear dependence of $\mathrm{Re}(\Lambda)_{\max}$ on $\varepsilon$ with $D_s=1$.

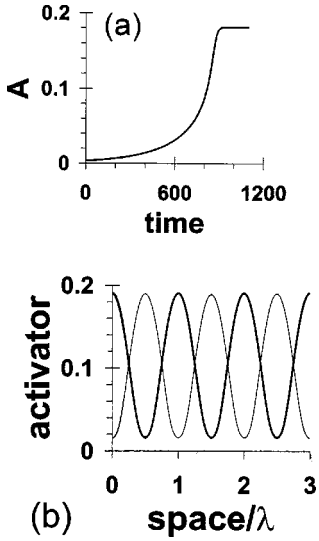


FIG. 3. Results of computer simulations. (a) Time dependence of the amplitude of standing waves at $\varepsilon=0.344$, where $\mathrm{Re}(\Lambda)_{\max}$ is positive (all other parameters as in Fig. 1) for small initial perturbation of the homogeneous steady state of the form $x_{SS}[1+0.01\cos(2\pi r/\lambda)]$ on a one-dimensional segment of length $L=3\lambda$ ($\lambda=2\pi/k_0$) with zero-flux boundary conditions; $r$ is the spatial coordinate. (b) Fully developed stationary standing waves in two antiphase states.

To underscore the difference between SWI and supercritical WI, we also show in Fig. 4 the behavior of $A$ in the case of supercritical WI, which is found in system (1–3) for $f>1$. In this case, $A$ depends on the bifurcation parameter [$\mathrm{Re}(\Lambda)$ or $(\varepsilon-\varepsilon_0)$] as in a typical second-order phase transition or supercritical Hopf bifurcation,[11] i.e., $A\propto\mathrm{Re}(\Lambda)^{1/2}$ or $A\propto(\varepsilon-\varepsilon_0)^{1/2}$.

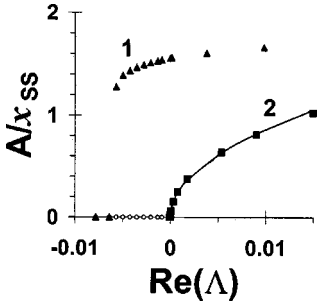


FIG. 4. Dependence of the amplitude ($A$) of standing waves on $\mathrm{Re}(\Lambda)_{\max}$ ($\varepsilon$ is varied) for subcritical (1) and supercritical (2) wave instability obtained by computer simulation of model (1–3). Parameters: $q=0.002$, $D_x=D_z=0.1$, $D_s=1$, $f=$(1) 0.92, (2) 1.1; $\beta=$(1) 0.4, (2) 0.38; $\varepsilon_2=$(1) 1.2, (2) 2. Symbols denote amplitudes found in simulations; computed points (squares) are fitted by smooth curve 2 as $A=0.2713[\mathrm{Re}(\Lambda)]^{1/2}$. Zero amplitudes, denoted by open circles, are obtained with small perturbations of the steady state at negative $\mathrm{Re}(\Lambda)_{\max}$. Large amplitudes denoted by triangles (curve 1) are obtained from standing waves developed at positive $\mathrm{Re}(\Lambda)_{\max}$ and further smooth increase [decrease] in $\varepsilon[\mathrm{Re}(\Lambda)_{\max}]$.

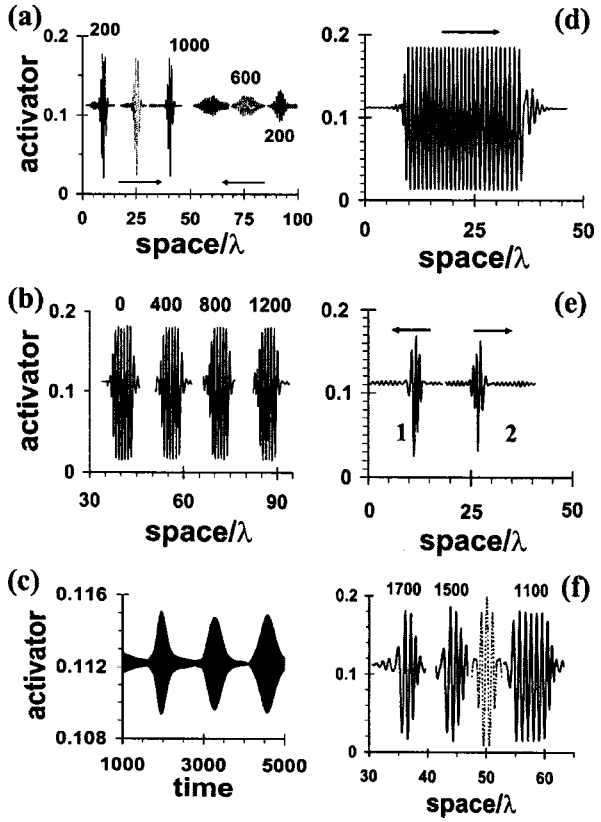


FIG. 5. Wave packets for SWI. All parameters except $\varepsilon$ as in Fig. 1. (a) Large- and small-amplitude wave packets. Arrows show direction of propagation; numbers above wave packets indicate corresponding times; $\varepsilon = 0.3465$; the amplitudes of small-amplitude wave packets are shown $\times 10$, i.e., quantity plotted is $10(x - x_{SS}) + x_{SS}$. (b) Propagation of large-amplitude wave packet at $\varepsilon = 0.346$. Initial wave packet was created at smaller $\varepsilon$. (c) Time behavior at $r = L/2$ when a small-amplitude wave packet travels on a segment of length $L = 50\lambda$ ($\lambda = 8.63$) at $\varepsilon = 0.3465$. (d) Rectangular large-amplitude wave packet, created at $\varepsilon = 0.34$, before collision with the zero-flux boundary, $L = 50\lambda$ ($\lambda = 8.63$), $\varepsilon = 0.3465$; (e) Resulting wave packet (1) after collision of the packet shown in (d) with the right boundary and before collision with the left boundary; (2) the same wave packet after collision with the left boundary, $\varepsilon = 0.3465$. (f) Collision of two large-amplitude wave packets at $\varepsilon = 0.346$. The initial wave packets (at $t = 1100$) were created at $\varepsilon = 0.344$. Only one wave packet is shown. The system is symmetric about $r = L/2 = 50\lambda$. Dotted curve shows collision of two identical packets in the center of the segment at $t = 1350$.

## III. PACKET WAVES

Another pattern associated with WI, packet waves, also exhibits new features at small, but positive $\mathrm{Re}(\Lambda)_{\max}$ [at negative $\mathrm{Re}(\Lambda)_{\max}$, all wave packets disappear] when the bifurcation is subcritical. We have found two types of wave packets, one with large amplitude (almost equal to the amplitude of standing waves) and the other with small amplitude [Fig. 5(a)].

The large-amplitude wave packet (LAWP) has an almost rectangular shape and propagates without spreading, like a soliton.[18–20] Its velocity (group velocity $v_g$) is given by $d\,\mathrm{Im}(\Lambda)/dk$ at $k = k_0$ (curve 4 in Fig. 1). The number of waves (phase waves) in the packet can take any integer value. Wave packets with large numbers of waves can be created at large (small) $\mathrm{Re}(\Lambda)_{\max}(\varepsilon)$, and their propagation can be studied at smaller (larger) $\mathrm{Re}(\Lambda)_{\max}(\varepsilon)$, close to the supercritical bifurcation point.

The small-amplitude wave packet (SAWP), created by a small localized perturbation of the steady state, has a Gaussian shape[21] and broadens as it propagates. These features can be seen in Fig. 5(c), which shows oscillations in the concentration of the activator $x$ [period $T = 2\pi/\mathrm{Im}(\Lambda) \cong 7.13$ at $k = k_0$] at $r = L/2$ during three passages of the wave packet through this point. The shape of these three peaks in time reflects the shape of the packet in space, and the width of a peak at half height multiplied by $v_g$ is approximately equal to the spatial width of the wave packet at the corresponding time. SAWPs colliding with boundaries (reflection) and with each other (passing through) behave the same way as in the case of supercritical WI.[15,22] The amplitude of a SAWP depends on the initial perturbation and should change with time as $t^{-1/2}\exp(pt)$, where $p \cong \mathrm{Re}(\Lambda)_{\max}$.[23] When $t > 0.5/p$, the amplitude starts to grow and the wave packet becomes unstable, transforming into a LAWP. Gaussian packet waves[21] are a collective behavior involving all spatial points. For this reason, the behavior of a wave packet depends on the total system size.

LAWPs created at large $\mathrm{Re}(\Lambda)_{\max}$ (or by a large amplitude localized initial perturbation) and propagating at smaller $\mathrm{Re}(\Lambda)_{\max}$ do not change their shape during propagation [Fig. 5(b)], but do change shape upon collision with boundaries and/or with other LAWPs [Figs. 5(d) and 5(f)]. In this sense, they can be called metastable. When broad rectangular LAWPs collide with each other [Fig. 5(f)], they are transformed into narrow LAWPs. Figure 5(d) shows a broad wave packet that propagates toward the right boundary at $r = 50\lambda$. After collision with and reflection from the boundary, the wave packet transforms into a narrow (one large peak) LAWP, which propagates unchanged [curve 1, Fig. 5(e)] toward the left boundary. This wave packet does not change shape after reflection from the boundary (curve 2) and continues to propagate unchanged for long times, $t \gg 1/\mathrm{Re}(\Lambda)_{\max}$, through multiple reflections from the boundaries.

Small-amplitude oscillations that emerge behind a large amplitude, solitonlike wave packet could, in principle, grow with a rate equal to the positive $\mathrm{Re}(\Lambda)_{\max}$ and give rise to large-amplitude standing waves, but this does not take place in a typical finite system, because the characteristic time of their growth, $1/\mathrm{Re}(\Lambda)_{\max}$, is larger than the return time of wave packets, which is given by $L/v_g$. When a LAWP propagates in the opposite direction after reflection from a boundary, it swamps out any small-amplitude waves, preventing them from growing. The fact that the LAWP remains unchanged by collision with small amplitude waves confirms that this packet is stable against small-amplitude perturbations. So, if $1/\mathrm{Re}(\Lambda)_{\max} > L/v_g$, LAWP represents a stable solution for zero-flux boundary conditions, as well as for periodic boundary conditions, in which case we have circulation of a solitonlike wave packet.

The wavelengths and group velocities of small- and large-amplitude wave packets are approximately the same, $2\pi/k_0$ and $d\,\mathrm{Im}(\Lambda)/dk$, respectively. The period of oscillation and the phase velocity of these wave packets are also equal: $2\pi/\mathrm{Im}(\Lambda)$ and $\mathrm{Im}(\Lambda)/k$ at $k = k_0$, respectively. The two types of packets are differentiated by the amplitude of

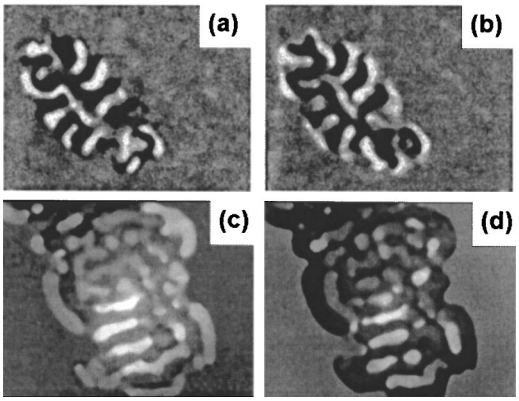


FIG. 6. Localized standing waves in the BZ-AOT system sandwiched between two flat glass windows (thickness of the reactive layer is 0.1 mm). Concentrations of initial reactants in the aqueous phase: (a, b) $[\text{malonic acid}]_0=0.3M$, $[H_2SO_4]_0=0.2M$, $[NaBrO_3]_0=0.2M$, $[\text{ferroin}]_0=4$ mM; volume fraction of droplets (with a surfactant shell) $\varphi_d=0.5$, $\omega\equiv[H_2O]/[\text{AOT}]=15$. Time between snapshots (a) and (b) is 30 s, and frame size $=2.3\times3$ mm$^2$. For (c) and (d) $[\text{malonic acid}]_0=0.4M$, $[H_2SO_4]_0=0.27M$, $[NaBrO_3]_0=0.3M$, $[Br]_0=0.042M$, [bathoferroin] $=4$ mM, $\varphi_d=0.31$, $\omega=14.15$. Time between snapshots (c) and (d) is 45 s, and frame size $=3.75\times5$ mm$^2$.

the waves, their shape, the spreading speed (dependence of packet width at half height on time), and behavior on collision with boundaries or with each other.

## IV. DISCUSSION

In quantum mechanics, unlike wave packets in reaction-diffusion systems, the amplitude of a Gaussian wave packet, a solution of the time-dependent Schrödinger equation,[21] has no physical meaning, since all physically meaningful expectation values contain the normalization factor $1/|\psi|^2$. Also, all solutions of the complex Ginsburg-Landau equation (CGLE) with purely imaginary coefficients are marginally stable.[19] This is a result of the fact that these equations describe Hamiltonian (conservative) systems. In contrast, for dissipative reaction-diffusion systems with positive $\text{Re}(\Lambda)$ the amplitude of a wave packet is an observable quantity.

We have shown here that the wave instability in reaction-diffusion systems may be subcritical, and we have demonstrated how systems with SWI may be constructed. Although an analytical criterion exists for the occurrence of the subcritical Hopf instability,[11,24] it is not yet possible to predict, without integrating the partial differential equations, which type of WI exists in any particular system. The phenomenological quintic CGLE allows one to describe a subcritical Hopf bifurcation,[19,25] and a CGLE coupled with a slow real mode[26] can produce a wave instability. Combining these equations, it is possible to write a coupled CGLE that can generate a subcritical wave instability. Analysis of such a coupled CGLE and examination of its relation to actual reaction-diffusion systems have yet to be performed.

SWI may occur in the packet waves[4] or antispirals[17] observed in the BZ-AOT system, where models similar to Eqs. (1)–(3) provide a reasonable description of the system. Figure 6 demonstrates large-amplitude localized standing waves observed in the BZ-AOT system at several different sets of experimental conditions (descriptions of the experimental configuration and methods of preparation of the BZ-AOT system can be found elsewhere[4]). In all cases shown, the pattern emerges suddenly. The background remains homogeneous and the area occupied by standing waves slowly expands. Unfortunately, our batch experiments do not allow us to resolve definitively whether these patterns arise from a subcritical wave instability or from a supercritical wave instability with slowly changing reactant concentrations. The former interpretation is supported by the fact that we were only able to observe these localized patterns with large amplitudes and never saw the increase in pattern amplitude that would be expected to accompany a supercritical bifurcation.

The amplitude of the LAWP in our model is two to three times smaller than the amplitude of the trigger waves in the corresponding two-variable model (1,2). In our BZ-AOT experiments, we find approximately the same ratio between the amplitudes of trigger and of packet or standing waves. SWI may also play a significant role in the localized oscillatory patterns (oscillons) found recently in the BZ-AOT system,[14] since in the range of negative $\text{Re}(\Lambda)_{\max}$, when $\varepsilon_W<\varepsilon<\varepsilon_{SW}$, two different patterns are stable.

Survival of two narrow solitonlike wave packets upon collision is analogous to the intriguing phenomenon in which two oncoming metabolic waves in living neutrophils[27] pass through one another. Trigger waves in systems close to a subcritical Hopf instability can also undergo collision with subsequent survival.[18] It appears that subcriticality may be intimately related with this solitonlike behavior of chemical waves in reaction-diffusion systems.

## ACKNOWLEDGMENT

This work was supported by Grant No. CHE-0306262 from the National Science Foundation.

[1] M. C. Cross and P. C. Hohenberg, Rev. Mod. Phys. **65**, 851 (1993).
[2] A. M. Turing, Philos. Trans. R. Soc. London, Ser. B **237**, 37 (1952).
[3] A. M. Zhabotinsky, M. Dolnik, and I. R. Epstein, J. Chem. Phys. **103**, 10306 (1995).
[4] V. K. Vanag and I. R. Epstein, Phys. Rev. Lett. **88**, 088303 (2002).
[5] P. Borckmans, G. Dewel, A. De Wit *et al.*, Int. J. Bifurcation Chaos Appl. Sci. Eng. **12**, 2307 (2002).
[6] A. De Wit, Adv. Chem. Phys. **109**, 435 (1999).
[7] V. K. Vanag and I. R. Epstein, Science **294**, 835 (2001).
[8] V. K. Vanag and I. R. Epstein, Phys. Rev. Lett. **87**, 228301 (2001).
[9] *Oscillations and Traveling Waves in Chemical Systems*, edited by R. J. Field and M. Burger (Wiley, New York, 1985).
[10] O. Jensen, V. O. Pannbacker, G. Dewel, and P. Borckmans, Phys. Lett. A **179**, 91 (1993).
[11] J. E. Marsden and M. McCracken, *The Hopf Bifurcation and its Applications* (Springer, New York, 1976).
[12] P. W. Davies, P. Blanchedeau, E. Dulos, and P. De Kepper, J. Phys. Chem. A **102**, 8236 (1998).
[13] O. Jensen, V. O. Pannbacker, E. Mosekilde, G. Dewel, and P. Borckmans, Phys. Rev. E **50**, 736 (1994).
[14] V. K. Vanag and I. R. Epstein, Phys. Rev. Lett. **92**, 128301 (2004).
[15] V. K. Vanag and I. R. Epstein, J. Phys. Chem. A **106**, 11394 (2002).
[16] F. Buchholtz, M. Dolnik, and I. R. Epstein, J. Phys. Chem. **99**, 15093 (1995).
[17] Y. Gong and D. J. Christini, Phys. Rev. Lett. **90**, 088302 (2003).
[18] J. Kosek and M. Marek, Phys. Rev. Lett. **74**, 2134 (1995).
[19] S. Fauve and O. Thual, Phys. Rev. Lett. **64**, 282 (1990).
[20] N. J. Zabusky and M. D. Kruskal, Phys. Rev. Lett. **15**, 240 (1965).
[21] J. A. Yeazell, and T. Uzer, *The Physics and Chemistry of Wave Packets* (Wiley, New York, 2000).

[22] L. F. Yang and I. R. Epstein, J. Phys. Chem. A **106**, 11676 (2002).
[23] J. D. Murray, *Mathematical Biology* (Springer, Berlin, 1989).
[24] J. Guckenheimer and P. Holmes, *Nonlinear Oscillations, Dynamical Systems, and Bifurcations of Vector Fields* (Springer, New York, 1983).
[25] W. van Saarloos and P. C. Hohenberg, Physica D **56**, 303 (1992).
[26] M. Ipsen and P. G. Sørensen, Phys. Rev. Lett. **84**, 2389 (2000).
[27] H. R. Petty and A. L. Kindzelskii, Proc. Natl. Acad. Sci. U.S.A. **98**, 3145 (2001).